

See discussions, stats, and author profiles for this publication at: <https://www.researchgate.net/publication/275215384>

# Tunable Surface Wettability of ZnO Nanoparticle Arrays for Controlling the Alignment of Liquid Crystals

ARTICLE in ACS APPLIED MATERIALS & INTERFACES · APRIL 2015

Impact Factor: 6.72 · DOI: 10.1021/acsaami.5b01157 · Source: PubMed

---

CITATION

1

---

READS

27

## 4 AUTHORS, INCLUDING:



[Mu-Zhe Chen](#)

National Chiao Tung University

3 PUBLICATIONS 6 CITATIONS

[SEE PROFILE](#)



[Sheng-Hsiung Yang](#)

National Chiao Tung University

30 PUBLICATIONS 2,134 CITATIONS

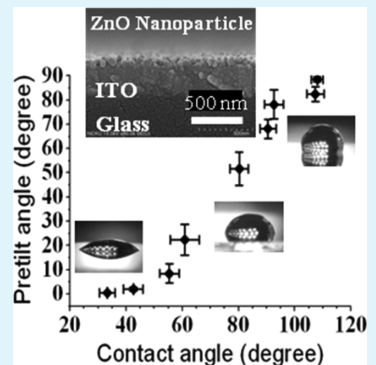
[SEE PROFILE](#)

# Tunable Surface Wettability of ZnO Nanoparticle Arrays for Controlling the Alignment of Liquid Crystals

Yueh-Feng Chung,<sup>†</sup> Mu-Zhe Chen,<sup>†</sup> Sheng-Hsiung Yang,<sup>‡</sup> and Shie-Chang Jeng<sup>\*,§</sup>

<sup>†</sup>Institute of Photonics System, <sup>‡</sup>Institute of Lighting and Energy Photonics, and <sup>§</sup>Institute of Imaging and Biomedical Photonics, National Chiao Tung University, Tainan 711, Taiwan

**ABSTRACT:** The control of the liquid crystal (LC) alignment is very important for both academic research and practical applications. LC molecules aligned on the ZnO nanoparticle arrays (ZnO NPAs) are demonstrated and the pretilt angles of LCs can be controlled by using ZnO NPAs with different surface wettability. The wettability of ZnO NPAs fabricated by the solution-based hydrothermal method can be controlled by changing the annealing temperature of the as-prepared ZnO NPAs. The measurements of the energy-dispersive spectra and photoluminescence have shown that the chemical properties of ZnO NPAs have been changed with the annealing temperature. Our results show that the pretilt angle of LCs can be tuned continuously from  $\sim 0$  to  $\sim 90^\circ$  as the contact angle of water on ZnO NPAs changes from 33 to  $108^\circ$ .



**KEYWORDS:** ZnO nanoparticle arrays, liquid crystal alignment, pretilt angle, wettability

## 1. INTRODUCTION

The control of liquid crystal (LC) molecules on solid alignment films is very important for both fundamental research and industrial applications. LC alignment is determined by the chemical interactions between the alignment film and the LC molecules, as well as the interplay between the anisotropic elastic properties of LCs and the morphology of the alignment film.<sup>1–4</sup> The alignment films are applied to orientate the LC molecules with a specific pretilt angle, the angle between the director of the LC molecules and the alignment films. LC devices (LCDs) with uniform alignment and appropriate pretilt angle are essential to obtain well-behaved electro-optical performances. The pretilt angles for the conventional homogeneous and homeotropic alignments are near 0 and  $90^\circ$ , respectively. Although the techniques for producing homogeneous (planar) and homeotropic (vertical) alignment by using rubbed polyimide (PI) films are mature in the LCDs industry, LCDs require different pretilt angles to show different electro-optical properties. For example, the fast no-bias optically compensated bend (OCB) LCD and the bistable bend-splay (BBS) LCD require the pretilt angles in the range of  $45^\circ$ – $60^\circ$ .<sup>5,6</sup>

There are many approaches that have been developed to control the pretilt angle of LCs, such as obliquely evaporated silicon monoxide,<sup>7</sup> photo induced polymerization of reactive monomer,<sup>8,9</sup> mixing of different materials,<sup>10–13</sup> and chemical synthesis.<sup>14,15</sup> However, the reliability of materials and ease of chemical synthesis for those proposed methods are questionable. It is complicated to synthesize the PI material with a specific pretilt angle, and the reliability of organic PI operated at high temperature and ultraviolet irradiation is still a problem.<sup>16</sup>

Recently, our group and Lim et al. found that the LC molecules can be aligned vertically to the ZnO nanowire arrays synthesized by the solution-based hydrothermal method.<sup>17,18</sup> This method shows the advantages of low cost, low manufacturing temperature, and well-controlled nanostructure on different substrates.<sup>19,20</sup> Several technologies have also been developed for applying nanomaterials as alignment films, such as the nanoporous anodic aluminum oxide (np-AAO) films,<sup>21,22</sup> the LC layer dispersed with nanoparticles<sup>23</sup> and the nano-rubbing of PI films by an atomic force microscope (AFM).<sup>24</sup> However, the control of pretilt angle by using np-AAO films is only  $\sim 2^\circ$ , and the mass production capability of the nanorubbing technique is questionable.

Applications of inorganic ZnO films for LC alignment are very promising for LCD systems operated in severe conditions. Photoinduced wettability transitions of ZnO nanostructured films from superhydrophobic surfaces to superhydrophilic surfaces have been investigated.<sup>25</sup> In this work, we report that the wettability of the ZnO nanoparticle arrays (ZnO NPAs) grown by the solution-based hydrothermal process can be modified by annealing temperature. The measurements of the energy dispersive spectra (EDS) and photoluminescence (PL) have shown that the chemical properties of ZnO NPAs have changed with the annealing temperature. Many studies in LC alignment films have shown that the pretilt angle of LC directors on alignment films strongly depends on their surface wettability.<sup>9,13,26–28</sup> Therefore, it is expected that the pretilt angle of the LC molecules can be controlled by adjusting the

Received: February 7, 2015

Accepted: April 20, 2015

surface property of the proposed ZnO NPAs films. Our results show that the pretilt angle of LCs is a function of the contact angle (CA) of water on the ZnO NPAs, and it can be tuned continuously over a wide range from 0.5 to 88.5° as the CA of water changes from 33 to 108°.

## 2. RESULTS AND DISCUSSION

**2.1. Morphology of ZnO NPAs.** The ZnO NPAs were synthesized by the hydrothermal method with the two-step process. A sol–gel solution comprising zinc acetate dihydrate and 2-(dimethylamino)ethanol in isopropanol was first spin-cast into thin film, followed by calcination at 200 °C in air to form the ZnO seed layer on the ITO glass substrate. In the second step, the substrate with the ZnO seed layer was immersed in a precursor bath, allowing the association of  $Zn^{2+}$  and  $OH^-$  for depositing  $Zn(OH)_2$  on the seed layer to form nanoparticle arrays, that were converted to final ZnO NPAs by thermal annealing at various temperatures.

Annealing studies were performed on the as-prepared ZnO NPAs at different temperatures. The nanostructure and the morphology of the ZnO NPAs observed by a scanning electron microscope (SEM) are shown in Figure 1, where we only show

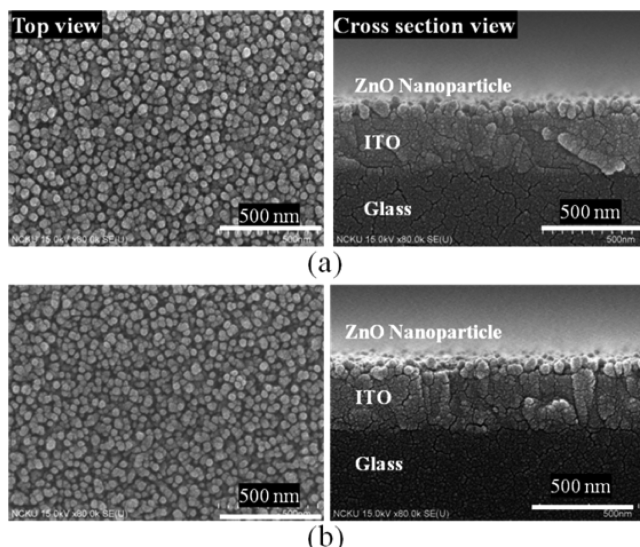


Figure 1. SEM images of ZnO NPAs annealed at two different temperatures: (a) 170 and (b) 300 °C.

the lowest (170 °C) and the highest annealing temperatures (300 °C) for comparison. In this work, we controlled the fabrication process especially the growth time for obtaining the particle-like geometry rather than the nanowire arrays used in our previous work.<sup>17</sup> The surface of the ZnO NPAs alignment film was also subjected to rubbing treatment before assembling antiparallel LC cells. It can be seen that most of ZnO nanoparticle grew regularly on the substrate with diameters of ~50 nm as shown in the top view of Figure 1. The thickness of the seed layer is less than 20 nm, and it is barely visible in Figure 1. For the ZnO NPAs with mechanical rubbing process, the topographic grooves are seen as shown in Figure 2, which are crucial for obtaining unidirectional LC alignment.

**2.2. Structural Property of ZnO NPAs.** The typical X-ray diffraction (XRD) patterns of as-prepared ZnO NPAs on the glass substrate annealed at 170 °C are shown in Figure 3. The observed intensity is weak because of the very thin ZnO NPAs

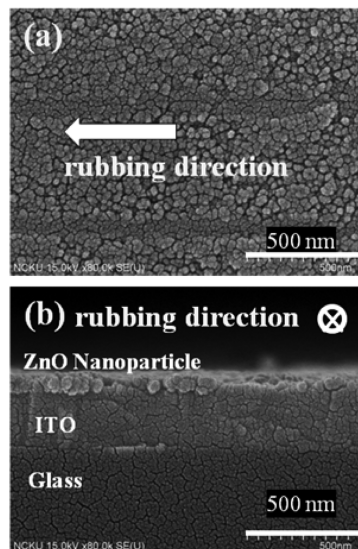


Figure 2. SEM images of a typical rubbed-ZnO NPAs. (a) Top view and (b) cross-section view.

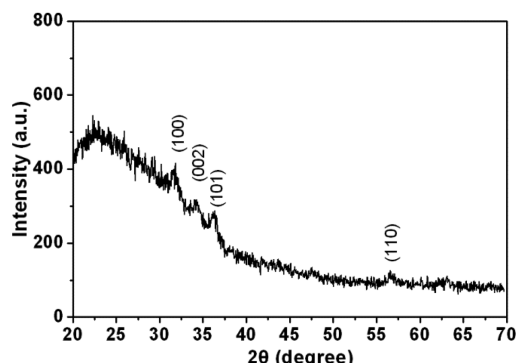
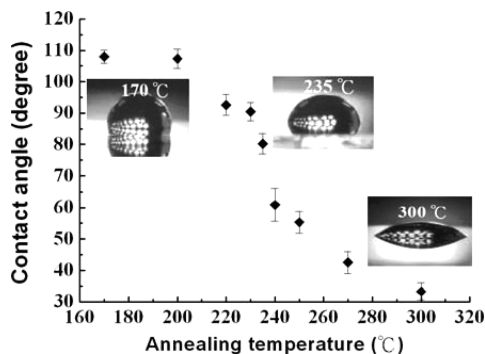


Figure 3. XRD patterns of ZnO NPAs annealed at 170 °C.

(~50 nm).<sup>29</sup> The XRD patterns are identified by using the standard powder diffraction data of ZnO, referred at JCPDS file no. 36–1451. The XRD patterns show three main peaks at around 31.7, 34.4, and 36.3°. These peaks represent the existence of hexagonal wurtzite structure of ZnO.

**2.3. Wettability of ZnO NPAs.** The wettability of rubbed-ZnO NPAs was evaluated by measuring the CA of water on their surfaces. The results of the CA of water drop on the ZnO NPAs prepared at different annealing temperatures are shown in Figure 4. It demonstrates that the CA decreases from 108° to 33° as the annealing temperature increases from 170 to 300 °C. The ZnO NPAs films show hydrophobic-like and hydrophilic-like surfaces at the low and high annealing temperatures, respectively. It means that the wettability of the ZnO NPAs is modified by the annealing process. The wettability of a solid surface is governed by both the chemical composition and the geometrical structure of the surface. The chemical composition of ZnO film relates to the defect chemistry and the surface crystal structure.<sup>30–38</sup> It is complex and it depends on the synthesis conditions, such as zinc source manufacturing temperature.<sup>30–38</sup>

**2.4. Chemical Properties of ZnO NPAs.** The EDS and the weight and atomic percent of zinc and oxygen elements of as-prepared ZnO NPAs films annealed at 170 and 300 °C are shown in Figure 5 and Table 1 for comparison, respectively. It indicates that the Zn/O ratio of the atomic percent slightly



**Figure 4.** Contact angle of water drop on ZnO NPAs films as a function of annealing temperature.

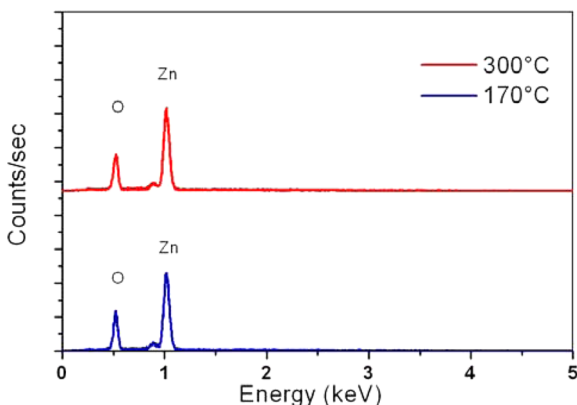


**Figure 5.** EDS of as-prepared ZnO NPA films annealed at 170 and 300 °C.

**Table 1. Weight Percent (wt %) and Atomic Percent (at %) of Zinc and Oxygen Elements in ZnO NPAs Films Annealed at 170°C and 300 °C**

	Zn (wt %)	Zn (at %)	O (wt %)	O (at %)
170 (°C)	73.7 ± 0.6	40.7 ± 0.7	26.3 ± 0.6	59.3 ± 0.7
300 (°C)	74.9 ± 0.3	42.2 ± 0.4	25.1 ± 0.3	57.8 ± 0.4

increases from 0.69 to 0.74 as the annealing temperature increases from 170 to 300 °C. Figure 6 shows the PL spectra of the as-prepared ZnO NPAs films annealed at 170 and 300 °C. The PL spectra of as-prepared ZnO NPAs films are featured by a strong band-edge UV emission from the free exciton recombination and a weak defect-related emission in the visible

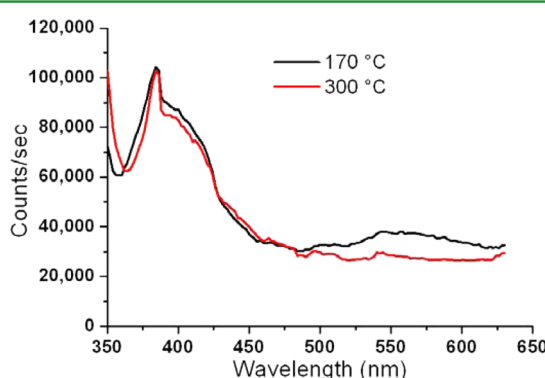


**Figure 6.** PL of ZnO NPA films annealed at 170 and 300 °C.

region. Defects in ZnO films are intrinsic properties and they depend on the growth conditions.<sup>30–38</sup> The possible intrinsic defects in ZnO films are oxygen vacancy, zinc vacancy, oxygen interstitial, zinc interstitial, oxygen antisite, and zinc antisite. Although the relationship between defect property and PL has been intensively studied in the literature, no consensus has been obtained regarding the origin of the different observed PL, mainly because of the different defect configurations in different samples.<sup>30–38</sup> As shown in Figure 6, a broad emission ~560 nm for ZnO NPAs annealed at 170 °C is clearly observed, and it decreases as the annealing temperature increases to 300 °C. The yellow emission is commonly attributed to interstitial oxygen defects<sup>33,36</sup> or the presence of Zn(OH)<sub>2</sub>.<sup>37</sup> A Zn(OH)<sub>2</sub> NPAs is initially obtained in the hydrothermal process. The Zn(OH)<sub>2</sub> gradually dehydrates to ZnO by annealing as the temperature increases from 100 °C to approximately 160 °C, the decomposition temperature of Zn(OH)<sub>2</sub>.<sup>30</sup> The reduced intensity of yellow emission from 170 to 300 °C may be attributed to the reduction of Zn(OH)<sub>2</sub> in the as-prepared ZnO NPAs. It was also reported that water vapor was chemisorbed on a ZnO surface at 300 °C and the excess of zinc at ZnO surfaces can react with water vapor to produce ZnO and hydrogen at a much higher temperature.<sup>36,38</sup> The studies of ZnO nanorods synthesized by electrodeposition also showed that the crystallinity of the ZnO increases with temperature from ~200 to ~300 °C, but point defects in the form of oxygen and zinc vacancies will also form as the annealing temperature increases above ~300 °C.<sup>30</sup> Both the chemisorbed water and possible oxygen defects in ZnO NPAs annealed at 300 °C may increase the surface wettability and surface energy of ZnO NPAs. Finally, the chemical properties of as-prepared ZnO films produce influence on the pretilt angle of LCs, which will be shown later.

**2.5. Pretilt Angles of LCs on ZnO NPAs.** The results of LC pretilt angle and CA of water as a function of the annealing temperature are both shown in Figure 7. It is observed that the

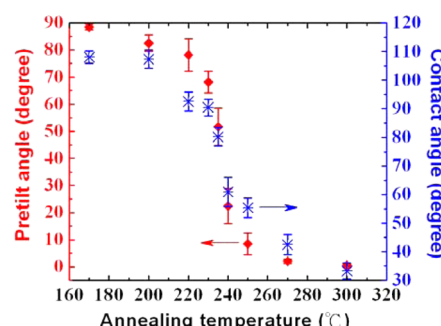


**Figure 7.** Pretilt angle of LCs and CA of water on ZnO NPAs film as a function of annealing temperature.

pretilt angle decreases from 88.5° to 0.5° along with an increase in the annealing temperature. Both the pretilt angle and the CA of water decrease as the annealing temperature increases, and these data are used to plot Figure 8, illustrating the change of the pretilt angle as a function of the CA. The pretilt angle rises from 0.5 to 88.5° as the CA of water changes from 33 to 108°. The results confirm that the pretilt angle strongly depends on the CA of water. In this work, we believe that the control of LC pretilt angle is caused by the different chemical surface properties of ZnO NPAs produced by different annealing temperatures. The semiempirical Friedel–Creagh–Kmetz

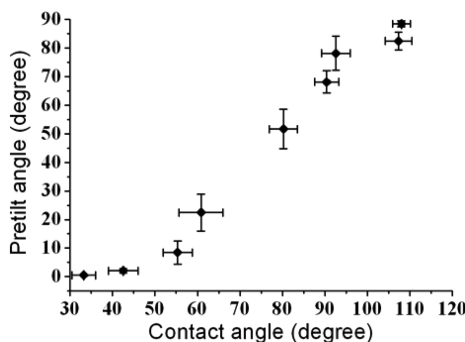


**Figure 8.** Pretilet angle of LCs as a function of CA of water on ZnO NPAs film.

(FCK) rule can be applied to show the relationship between the surface energy of an alignment film and LC orientation.<sup>39</sup> The FCK rule states that

$$\gamma_s < \gamma_{LC} \text{ homeotropic alignment}$$

$$\gamma_s > \gamma_{LC} \text{ homogenous alignment}$$

where  $\gamma_s$  describes the surface energy of the solid alignment film and  $\gamma_{LC}$  is the surface energy of the LCs. For example, the LC molecules favor vertical alignment on the solid film when the surface energy of the film is relatively low and the intermolecular interaction of LC molecules is stronger than the interaction across the interface. The surface energy of a solid film can be estimated by measuring the CA of water on the solid film according to the Girifalco–Good–Fowkes–Young model.<sup>40</sup> In general, a lower CA of water corresponds to a higher surface energy and vice versa. The FCK rule has been widely supported by experimental data.<sup>9,13,25–28,39</sup> In our case shown in Figure 8, the pretilt angle rises from  $\sim 0.5^\circ$  (homogeneous alignment) to  $\sim 88.5^\circ$  (homeotropic alignment) as the CA of water changes from  $\sim 33^\circ$  (high surface energy) to  $\sim 108^\circ$  (low surface energy). Our results follow the FCK rule.

**2.6. Electro-optical Properties of LCDs.** The polarizing optical microscope (POM) photographs of antiparallel LC cells with ZnO NPAs alignment films annealed at different temperatures are shown in Figure 9. The LC cells with different color represent the different pretilt angles corresponding to the different phase retardations. The phase retardations of antiparallel LC cells with ZnO NPAs alignment films annealed at different temperatures operated at different driving voltages are shown in Figure 10.

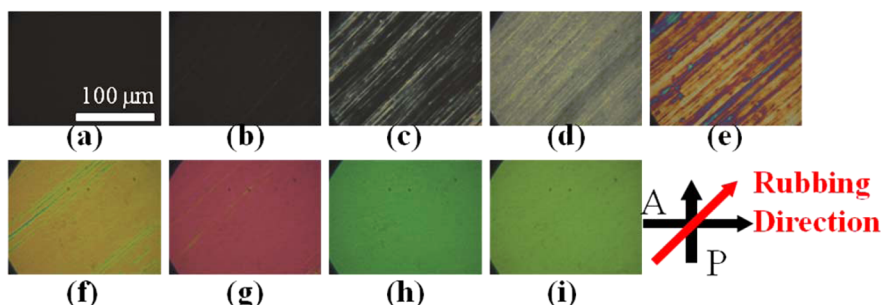


**Figure 9.** POM photographs of antiparallel LC cells with ZnO NPAs alignment films annealed at different temperatures: (a) 170, (b) 200, (c) 220, (d) 230, (e) 235, (f) 240, (g) 250, (h) 270, and (i) 300 °C.

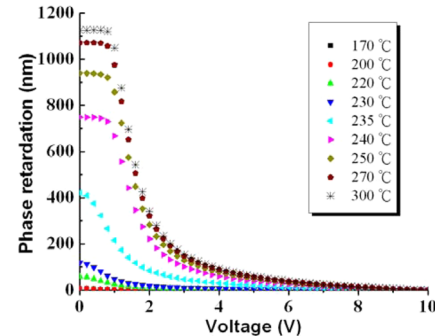


**Figure 10.** Phase retardation curves of antiparallel LC cells with ZnO NPAs alignment films annealed at different temperatures as a function of applied voltage.

In the voltage-off state, the LC molecules are aligned by ZnO NPAs with a pretilt angle  $\theta_p$ , meaning that the maximum phase retardation  $\Gamma_{\max}$  of the LC cell equals  $\Gamma_{\max} = (2\pi/\lambda)(n_e^{\text{eff}} - n_o)d$ .

Here,  $n_e^{\text{eff}} = ((n_e n_o)/(n_e^2 \sin^2 \theta_p + n_o^2 \cos^2 \theta_p)^{1/2})$ , where  $n_e$  and  $n_o$  are the extraordinary and ordinary refractive indices of the LC material, respectively. Therefore, the LC cell with the lower pretilt angle ( $\sim 0^\circ$ ) has the larger  $\Gamma_{\max}$  in the voltage-off state. Figure 10 illustrates that the maximum phase retardation  $\Gamma_{\max}$  in the voltage-off state increases with the temperature, indicating that the pretilt angle of LCs decreases from  $\sim 90^\circ$  to  $\sim 0^\circ$  as the temperature increases. These results agree with the results shown in Figures 7 and 9.

The transmittance of the ITO layer is important for LCDs applications. We have investigated the influence of annealing on the transmittance of ITO glass substrates as shown in Figure 11. The transmittance has no significant change in the visible range for different annealing temperatures. The transmittance only shows a small decrease of  $\sim 4\%$  around 420–450 nm.

Alignment materials with high thermal and photo stability are required for LCDs' applications.<sup>16,41</sup> Photostability of organic PI and inorganic silicon-dioxide ( $\text{SiO}_2$ ) alignment layers were studied by C.-H. Wen et al.<sup>16</sup> Their results indicated that  $\text{SiO}_2$  alignment layers are much more robust than conventional PI layers. A series of experiments for studying the reliability of the as-prepared ZnO films under high temperature and UV light is in progress. The electro-optical properties and the density of impurity ions of aged-LC cells will be measured for evaluating the reliability. It is expected that our proposed inorganic ZnO films can show similar reliability as  $\text{SiO}_2$  films.

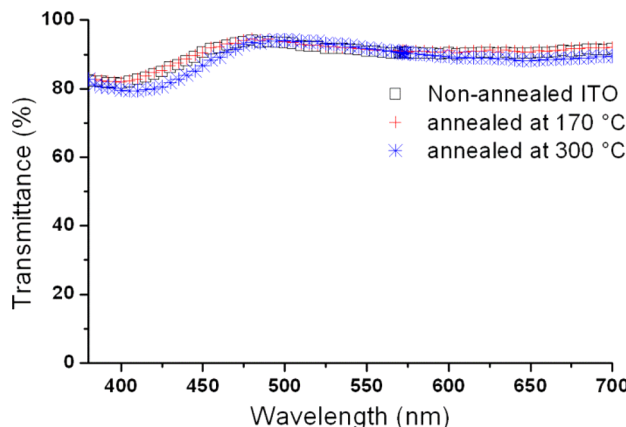


**Figure 11.** Transmittance spectra of the ITO glass substrates annealed at 170 and 300 °C compared with a nonannealed one.

### 3. CONCLUSION

The present study confirms that annealing treatment can be applied to modify the chemical property of the ZnO NPAs prepared by the solution-based hydrothermal method, and it has been applied successfully for LCDs with controllable pretilt angles. The measurements of the EDS and PL have shown that the chemical properties of ZnO NPAs have changed with the annealing temperature. The relationship between surface wettability of ZnO NPAs and LC pretilt angle is investigated. We find that the pretilt angle strongly depends on the surface wettability. The pretilt angle of LCs can be tuned continuously from 0.5 to 88.5° as the CA of water changes from 33 to 108°. The proposed method for controlling the pretilt angle of LCs is very simple and may provide a reliable inorganic alignment material for LCDs operated in a severe environment.

### 4. METHODS

**Materials.** In this research, we demonstrate the preparation and thermal treatment of ZnO NPAs that were grown vertically on indium tin oxide (ITO)/glass substrates for the LC alignment. A thin layer of textured ZnO seeds was first deposited on the ITO glass substrate, followed by growth of ZnO NPAs in the solution state. Detailed procedure for fabricating ZnO NPAs is described as follows.<sup>17</sup> A solution of zinc acetate dihydrate (0.22 g, 1 mmol) in 10 mL of isopropanol was slowly added to 2-(dimethylamino)ethanol (0.089 g, 1 mmol) within 5 min. The mixture was continuously stirred at 120 °C for 2 h until it became homogeneous and transparent. After cooling to room temperature, the formed solution was deposited into thin film on ITO glass substrate by spin-coating process, followed by calcination at 200 °C in air for 1 h to form a ZnO seed layer. To prepare the bath solution, we dissolved zinc sulfate heptahydrate (0.144 g, 0.5 mmol) and ammonium chloride (1.07 g, 20 mmol) in 50 mL of deionized water. The pH value of the solution was monitored by a pH meter and carefully adjusted to 10.3 by slowly adding 2 M NaOH aqueous solution. The bath solution was heated to 90 °C in an oven, and the ITO glass substrates coated with ZnO seed layers were immersed in the bath solution (ZnO seed layer downward) for 15 min to grow ZnO NPAs. If the growth time is increased, the grown nanostructure can become ZnO nanorods arrays or ZnO nanowire arrays. The substrates were sequentially washed with deionized water, acetone, and isopropanol, followed by annealing in air at different temperatures for 1 h to form the as-prepared ZnO NPAs. The annealing temperatures were set at 170, 200, 220, 230, 235, 240, 250, 270, and 300 °C. The surface of the ZnO NPAs with thermal treatment was then subjected to rubbing treatment once in each direction for forming the final alignment films.

**Sample Preparation.** To determine electro-optical properties of LC molecules on ZnO NPAs alignment films, the antiparallel LC cells were fabricated with a cell gap of ~5.1 μm and filled with LC molecules (E7,  $\Delta\epsilon = 14.1$ ,  $\epsilon_{\perp} = 5.2$ ,  $n_e = 1.74$ ,  $n_o = 1.52$ , Daily Polymer Corp.). Here, the rubbing directions of the two boundary alignment films for the antiparallel LC cells are antiparallel. During the LC filling, the LC cells were heated to a temperature above the clearing point ~65 °C to obtain uniform alignment.

**Measurements.** The morphology and EDS of ZnO NPAs was studied by using a SEM (SU8000, Hitachi) equipped with an X-ray detector (Xflash 5010, Bruker). To characterize the composition of the as-prepared ZnO films, EDS analysis was performed by using the 5 keV electrons for reducing the signal of oxygen from ITO glass substrate. Once the energy of electrons is too big, 10 keV for example, the signal of indium and oxygen from ITO glass can be observed (not shown here). The structure and crystallinity of ZnO was carried out by an XRD system (D/MAX-2500, Rigaku) using Cu-K $\alpha$  radiation source ( $\lambda = 1.54 \text{ \AA}$ ). The PL measurement was conducted by using a He-Cd laser for excitation (325 nm) at room temperature. The PL spectra were measured by a spectrometer (Acton SP2150) and recorded by a photomultiplier tube (PD471, Princeton Instruments). In order to reduce the PL from the ITO glass substrate, the excitation laser was near glancing incidence for reducing the laser power absorbed by the ITO film. The wettability of rubbed-ZnO NPAs was evaluated by measuring the CA of distilled water on their surfaces using a contact angle analyzer (CAM-100, Creating Nano Technologies). The pretilt angles of LCs were determined by the modified crystal rotation method,<sup>42</sup> where a laser interferometer (5530, Agilent) was used to determine the phase retardation.<sup>43</sup> The electro-optical properties of the LC cells were also studied by the POM (Olympus BX51) and phase retardation measurements.

### ■ AUTHOR INFORMATION

#### Corresponding Author

\*E-mail: scjeng@faculty.nctu.edu.tw.

#### Notes

The authors declare no competing financial interest.

### ■ ACKNOWLEDGMENTS

The authors thank the Ministry of Science and Technology of Taiwan for financially supporting this research under contract MOST 103-2112-M-009-013-MY3 and NSC102-2113-M-009-007.

### ■ REFERENCES

- (1) Geary, J. M.; Goodby, J. W.; Kmetz, A. R.; Patel, J. S. The Mechanism of Polymer Alignment of Liquid Crystal Materials. *J. Appl. Phys.* **1987**, *62*, 4100–4108.
- (2) Toney, M. F.; Russell, T. P.; Logan, J. A.; Kiguchi, H.; Sands, J. M.; Kumar, S. K. Near-Surface Alignment of Polymers in Rubbed Films. *Nature* **1995**, *374*, 709–711.
- (3) Berreman, D. W. Solid Surface Shape and the Alignment of an Adjacent Nematic Liquid Crystal. *Phys. Rev. Lett.* **1972**, *28*, 1683–1686.
- (4) Kumar, S.; Kim, J. H.; Shi, Y. What Aligns Liquid Crystals on Solid Substrates? The Role of Surface Roughness Anisotropy. *Phys. Rev. Lett.* **2005**, *94*, 077803.
- (5) Yeung, F. S. Y.; Kwok, H.-S. Fast-Response No-Bias-Bend Liquid Crystal Displays Using Nanostructured Surfaces. *Appl. Phys. Lett.* **2006**, *88*, 063505.
- (6) Yu, X. J.; Kwok, H.-S. Bistable Bend-Splay Liquid Crystal Display. *Appl. Phys. Lett.* **2004**, *85*, 3711–3713.
- (7) Uchida, T.; Ohgawara, M.; Wada, M. Liquid Crystal Orientation on the Surface of Obliquely-Evaporated Silicon Monoxide with Homeotropic Surface Treatment. *Jpn. J. Appl. Phys.* **1980**, *19*, 2127–2136.

- (8) Chen, T.-J.; Chu, K.-L. Pretilt Angle Control for Single-Cell-Gap Transflective Liquid Crystal Cells. *Appl. Phys. Lett.* **2008**, *92*, 091102.
- (9) Liu, B.-Y.; Chen, L.-J. Role of Surface Hydrophobicity in Pretilt Angle Control of Polymer-Stabilized Liquid Crystal Alignment Systems. *J. Phys. Chem. C* **2013**, *117*, 13474–13478.
- (10) Kwok, H.-S.; Yeung, F. S. Y. Nano-Structured Liquid-Crystal Alignment Layers. *J. Soc. Inf. Disp.* **2008**, *16*, 911–918.
- (11) Wu, W.-Y.; Wang, C.-C.; Fuh, A. Y.-G. Controlling Pre-Tilt Angles of Liquid Crystal Using Mixed Polyimide Alignment Layer. *Opt. Express* **2008**, *16*, 17131–17137.
- (12) Ahn, D.; Jeong, Y.-C.; Lee, S.; Lee, J.; Heo, Y.; Park, J.-K. Control of Liquid Crystal Pretilt Angles by Using Organic/Inorganic Hybrid Interpenetrating Networks. *Opt. Express* **2009**, *17*, 16603–16612.
- (13) Hwang, S.-J.; Jeng, S.-C.; Hsieh, I.-M. Nanoparticle-Doped Polyimide for Controlling the Pretilt Angle of Liquid Crystals Devices. *Opt. Express* **2010**, *18*, 16507–16512.
- (14) Nishikawa, M. Design of Polyimides for Liquid Crystal Alignment Films. *Polym. Adv. Technol.* **2000**, *11*, 404–412.
- (15) Lee, Y. J.; Choi, J. G.; Song, I. K.; Oh, J. M.; Yi, M. H. Effect of Side Chain Structure of Polyimides on a Pretilt Angle of Liquid Crystal Cells. *Polymer* **2006**, *47*, 1555–1562.
- (16) Wen, C.-H.; Gauza, S.; Wu, S.-T. Photostability of Liquid Crystals and Alignment Layers. *J. Soc. Inf. Disp.* **2005**, *13*, 805.
- (17) Chen, M.-Z.; Chen, W.-S.; Jeng, S.-C.; Yang, S.-H.; Chung, Y.-F. Liquid Crystal Alignment on Zinc Oxide Nanowire Arrays for LCDs Applications. *Opt. Express* **2013**, *21*, 29277–29282.
- (18) Lim, Y. J.; Choi, Y. E.; Kang, S.-W.; Kim, D. Y.; Lee, S. H.; Hahn, Y.-B. Vertical Alignment of Liquid Crystals with Zinc Oxide Nanorods. *Nanotechnology* **2013**, *24*, 345702.
- (19) Yamabi, S.; Imai, H. Growth Conditions for Wurtzite Zinc Oxide Films in Aqueous Solutions. *J. Mater. Chem.* **2002**, *12*, 3773–3778.
- (20) Vayssieres, L. Growth of Arrayed Nanorods and Nanowires of ZnO from Aqueous Solutions. *Adv. Mater.* **2003**, *15*, 464–466.
- (21) Maeda, T.; Hiroshima, K. Vertically Aligned Nematic Liquid Crystal on Anodic Porous Alumina. *Jpn. J. Appl. Phys.* **2004**, *43*, L1004–L1006.
- (22) Hong, C.; Tang, T.-T.; Hung, C.-Y.; Pan, R.-P.; Fang, W. Liquid Crystal Alignment in Nanoporous Anodic Aluminum Oxide Layer for LCD Panel Applications. *Nanotechnology* **2010**, *21*, 285201.
- (23) Qi, T.; Hegmann, T. Impact of Nanoscale Particles and Carbon Nanotubes on Current and Future Generations of Liquid Crystal Displays. *J. Mater. Chem.* **2008**, *18*, 3288–3294.
- (24) Ruetschi, M.; Grutter, P.; Funfschilling, J.; Guntherodt, H. J. Creation of Liquid Crystal Waveguides with Scanning Force Microscopy. *Science* **1994**, *265*, 512–4.
- (25) Feng, X. J.; Feng, L.; Jin, M. H.; Zhai, J.; Jiang, L.; Zhu, D. B. Reversible Super-Hydrophobicity to Super-Hydrophilicity Transition of Aligned ZnO Nanorod Films. *J. Am. Chem. Soc.* **2004**, *126*, 62–63.
- (26) Paek, S. H.; Durning, C. J.; Lee, K. W.; Lien, A. A Mechanistic Picture of the Effects of Rubbing on Polyimide Surfaces and Liquid Crystal Pretilt Angles. *J. Appl. Phys.* **1998**, *83*, 1270–1280.
- (27) Ban, B. S.; Kim, Y. B. Surface Free Energy and Pretilt Angle on Rubbed Polyimide Surfaces. *J. Appl. Polym. Sci.* **1999**, *74*, 267–271.
- (28) Ahn, H. J.; Kim, J. B.; Kim, K. C.; Hwang, B. H.; Kim, J. T.; Baik, H. K.; Park, J. S.; Kang, D. Liquid Crystal Pretilt Angle Control Using Adjustable Wetting Properties of Alignment Layers. *Appl. Phys. Lett.* **2007**, *90*, 253505.
- (29) Olson, T. Y.; Chernov, A. A.; Drabek, B. A.; Satcher, J. H., Jr.; Han, T. Y.-J. Experimental Validation of the Geometrical Selection Model for Hydrothermally Grown Zinc Oxide Nanowire Arrays. *Chem. Mater.* **2013**, *25*, 1363–1371.
- (30) Iza, D. C.; Munoz-Rojas, D.; Jia, Q. X.; Swartzentruber, B.; MacManus-Driscoll, J. L. Tuning of Defects in ZnO Nanorod Arrays Used in Bulk Heterojunction Solar Cells. *Nanoscale Res. Lett.* **2012**, *7*, 655.
- (31) McCluskey, M. D.; Jokela, S. J. Defects in ZnO. *J. Appl. Phys.* **2009**, *106*, 071101.
- (32) Li, D.; Leung, Y. H.; Djurišić, A. B.; Liu, Z. T.; Xie, M. H.; Shi, S. L.; Xu, S. J.; Chan, W. K. Different Origins of Visible Luminescence in ZnO Nanostructures Fabricated by the Chemical and Evaporation Methods. *Appl. Phys. Lett.* **2004**, *85*, 1601–1603.
- (33) Greene, L. E.; Law, M.; Goldberger, J.; Kim, F.; Johnson, J. C.; Zhang, Y. F.; Saykally, R. J.; Yang, P. D. Low-Temperature Wafer-Scale Production of ZnO Nanowire Arrays. *Angew. Chem., Int. Ed.* **2003**, *42*, 3031–3034.
- (34) Choi, M. H.; Ma, T. Y. Influence of Substrate Temperature on Ultraviolet Emission of ZnO Films Prepared by Ultrasonic Spray Pyrolysis. *J. Mater. Sci.* **2006**, *41*, 431–435.
- (35) Lin, C. C.; Hsiao, C. S.; Chen, S. Y.; Chen, S. Y. Ultraviolet Emission in ZnO Films Controlled by Point Defects. *J. Electrochem. Soc.* **2004**, *151*, G285–G288.
- (36) Liu, M.; Kitai, A. H.; Mascher, P. Point Defects and Luminescence Centres in Zinc Oxide and Zinc Oxide Doped with Manganese. *J. Lumin.* **1992**, *54*, 35–42.
- (37) Zhou, H.; Alves, H.; Hofmann, D. M.; Kriegseis, W.; Meyer, B. K.; Kaczmarsky, G.; Hoffmann, A. Behind the Weak Excitonic Emission of ZnO Quantum Dots: ZnO/Zn(OH)<sub>2</sub> Core-shell Structure. *Appl. Phys. Lett.* **2002**, *80*, 210–212.
- (38) Lukan, O.; Guerin, V. M.; Tiginianu, I. M.; Ursaki, V. V.; Chow, L.; Heinrich, H.; Pauporte, T. Well-aligned Arrays of Vertically Oriented ZnO Nanowires Electrodeposited on ITO-coated Glass and their Integration in Dye Sensitized Solar Cells. *J. Photochem. Photobiol. A* **2010**, *211*, 65–73.
- (39) Cognard, J. *Alignment of Nematic Liquid Crystals and Their Mixtures*; Gordon and Breach Science Publishers: New York, 1982.
- (40) Hiemenz, P. C.; Rajagopalan, R. *Principles of Colloid and Surface Chemistry*; Marcel Dekker: New York, 1997.
- (41) Ishihara, S. How Far Has the Molecular Alignment of Liquid Crystals Been Elucidated? *J. Disp. Technol.* **2005**, *1*, 30–40.
- (42) Chen, K.-H.; Chang, W.-Y.; Chen, J.-H. Measurement of the Pretilt Angle and the Cell Gap of Nematic Liquid Crystal Cells by Heterodyne Interferometry. *Opt. Express* **2009**, *17*, 14143–14149.
- (43) Hwang, S.-J. Precise Optical Retardation Measurement of Nematic Liquid Crystal Display Using the Phase-Sensitive Technique. *J. Disp. Technol.* **2005**, *1*, 77–81.